Comparison of Ground-Based Millimeter-Wave Observations and Simulations in the Arctic Winter

Domenico Cimini, Francesco Nasir, Ed R. Westwater, *Fellow, IEEE*, Vivienne H. Payne, David D. Turner, Eli J. Mlawer, Michael L. Exner, and Maria P. Cadeddu

***Abstract*—During the Radiative Heating in Underexplored Bands Campaign (RHUBC), held in February–March 2007, three millimeter-wave radiometers were operated at the Atmospheric Radiation Measurement Program's site in Barrow, Alaska. These radiometers contain several channels located around the strong 183.31-GHz water vapor line, which is crucial for ground-based water-vapor measurements in very dry conditions, typical of the Arctic. Simultaneous radiosonde observations were carried out during conditions with very low integrated-water-vapor (IWV) content ($<$ 2mm). Observations from the three instruments are compared, accounting for their different design characteristics. The overall agreement during RHUBC among the three instruments and between instruments and forward model is discussed quantitatively. In general, the instrument cross-validation performed for sets of channel pairs showed agreement within the total expected uncertainty. The consistency between instruments allows the determination of the IWV to within around 2% for these dry conditions. Comparisons between these data sets and forward-model simulations using radiosondes as input show spectral features in the brightness-temperature residuals, indicating some degree of inconsistency between the instruments and the forward model. The most likely cause of forward-model error is systematic errors in the radiosonde humidity profiles.**

***Index Terms*—Arctic regions, atmospheric measurements, radiometry.**

I. Introduction

ATMOSPHERIC water vapor plays a key role in the energy balance of the Earth. Accurate measurements are needed worldwide, including the very dry regions where the sensitivity of conventional instrumentation is limiting the development of radiative-transfer models [2]. In the last decade, a series of field campaigns held in the Arctic showed that millimeter-wave radiometry provides enhanced sensitivity to low water vapor and liquid amounts with respect to conventional microwave radiometry [2]–[4], [8]. More recently, three millimeter-wave radiometers were deployed during the Radiative Heating in Underexplored Bands Campaign (RHUBC), which was held in February–March 2007 at the U.S. Department of Energy (DOE) Atmospheric Radiation Measurement (ARM) Program's North Slope of Alaska (NSA) site in Barrow, Alaska [1]. The cold and dry conditions experienced during RHUBC can be expressed as follows: air temperature (at 2 m) ranging from -38 °C to -19 °C and integrated water vapor (IWV) content from 0.9 to 3.6 mm. The three instruments are the ground-based scanning radiometer (GSR), developed by the Center for Environmental Technology of the University of Colorado (CET/CU), the Microwave Profiler MP-183A, manufactured by Radiometrics, and the ARM G-band water-Vapor Radiometer (GVR), manufactured by ProSensing. From the same site, ARM operational radiosondes were routinely launched twice a day. These operational radiosondes were complemented by a large number of additional radiosondes that were released during dry conditions with low IWV content (IWV $<$ 2 mm), as detected by near-real-time GSR retrievals. The aim of the RHUBC experiment was to study radiative heating occurring in the far-infrared spectrum using accurate estimates of the water vapor content from independent and reliable sensors. The GSR, GVR, and MP-183A all have several channels located around the strong 183.31-GHz water vapor line, which was demonstrated to be very important for ground-based water-vapor measurements in very dry conditions [2], [3]. These instruments have been developed and improved since 2004 [4], and RHUBC offers the first opportunity to cross-check instrument performances and the quality of data taken during field experiments. The primary focus of the work presented in this paper was to assess the extent of the agreement between the three independent instruments. Observations from the three radiometers cannot be directly compared due to different design characteristics (center frequency, sideband type, bandpass, sampling times, etc.) but can still be compared indirectly in the brightness-temperature (Tb) space using a radiative-transfer model as a transfer function. The use of a model requires that all of the earlier design characteristics be incorporated.

In this paper, we compare the three original independent data sets using model simulations computed from radiosondes to account for the different characteristics of the GSR, GVR, and MP-183A instruments in order to quantify the overall agreement obtained during the experiment. We also

Manuscript received September 25, 2008; revised January 7, 2009 and February 20, 2009. First published July 10, 2009; current version published August 28, 2009. This work was supported in part by the Environmental Sciences Division of the U.S. Department of Energy under the Atmospheric Radiation Measurement (ARM) Program. The work of D. D. Turner at the University of Wisconsin-Madison was supported by ARM under Grant DE-FG02-06ER64167.

D. Cimini and F. Nasir are with the Center of Excellence for Remote Sensing and Modeling of Severe Weather, University of L'Aquila, 67100 L'Aquila, Italy (e-mail: nico.cimini@aquila.infn.it).

E. R. Westwater is with the Center for Environmental Technology, Department of Electrical and Computer Engineering, University of Colorado at Boulder, Boulder, CO 80309-0425 USA (e-mail: ed.westwater@colorado.edu).

V. H. Payne and E. J. Mlawer are with the Atmospheric and Environmental Research, Inc., Lexington, MA 02421 USA (e-mail: vpayne@aer.com; emlawer@aer.com).

D. D. Turner is with the Space Science and Engineering Center, University of Wisconsin-Madison, Madison, WI 53706 USA (e-mail: dturner@ssec.wisc.edu).

M. L. Exner is with the Radiometrics Corporation, Boulder, CO 80301 USA (e-mail: exner@radiometrics.com).

M. P. Cadeddu is with the Argonne National Laboratory, Argonne, IL 60439 USA (e-mail: mcadeddu@anl.gov).

Digital Object Identifier 10.1109/TGRS.2009.2020743

TABLE I
MAIN CHARACTERISTICS OF THE THREE MILLIMETER-WAVE RADIOMETERS DEPLOYED DURING RHUBC

	GSR	GVR	MP-183A
Receiver Type	Filter bank	Filter bank	Frequency agile
Side Band	Double	Double	Single
Calibration	2 internal loads 2 external targets Tip curve	2 external targets	1 internal load 1 external target Tip curve
Channels	27 (7 around 183 GHz)	4	15
	183.31 ± 0.55 183.31 ± 1.0 183.31 ± 3.05 183.31 ± 4.7 183.31 ± 7.0 183.31 ± 12 183.31 ± 16	183.31 ± 1.0 183.31 ± 3.0 183.31 ± 7.0 183.31 ± 14.0	183.31 183.00 182.00 181.00 180.00 179.00 178.00 177.00 176.00 175.00 174.00 173.00 172.00 171.00 170.00

discuss discrepancies between measurements and forward-model simulations.

II. INSTRUMENTATION

A. GSR

The GSR is a 27-channel instrument designed and developed by CET/CU [4]. The frequency range spans from 50 to 400 GHz, although only the seven channels near the 183.31-GHz water vapor line are used in this paper (Table I). The first deployment of the GSR was in 2004 at the ARM NSA site [2]. The GSR deploys a filter-bank-type receiver with double-side passband filters. Using manufacturer specifications and data from the WVIOP2004, an equivalent monochromatic frequency (EMF) was determined for each GSR channel, resulting in Tb-modeling errors within 0.1 K with respect to the band-averaged values [11]. As described in [4], the calibration procedure for GSR relies on a combination of internal loads, external targets, and tipping curve, achieving an estimated accuracy of 1.0–1.5 K depending upon channel.

B. GVR

More recently, DOE funded the development of the GVR, a four-channel GVR designed and developed by ProSensing [5]. The GVR has been operating continuously since its first deployment at the ARM NSA site in April 2005 [3]. The four channels of the GVR are all distributed around 183.31 GHz (Table I); the filter-bank-type receiver has double-side passband filters of 0.5, 1.0, 1.4, and 2.0 GHz for the 183.31 ± 1-, 3-, 7-, 14-GHz channels, respectively. The spectral shape of the passband filters mounted on the GVR is shown in [5]. However, note that the passband measurements were collected not from the actual GVR but from an identical component mounted on another unit. The calibration of the GVR relies on external (to the antenna horn) hot/cold targets, leading to an estimated accuracy within 2 K [3], [5].

C. MP-183A

Even more recently, DOE funded the development of another G-band radiometer, designed and developed by Radiometrics. The frequency-agile Microwave Profiler MP-183A has over 1000 tunable channels, of which 15 from 170 to 183.31 GHz were calibrated for RHUBC (Table I). The MP-183A bandwidth is determined by an eight-pole intermediate frequency (IF) filter, characterized by sharp cutoffs. The 3-dB bandwidth IF bandpass filter is nominally 25–500 MHz, although the actual measured bandwidth is slightly wider. Thus, the effective RF bandwidth is 1118 MHz with a 30-MHz notch in the middle and is virtually identical for all channels. Concerning the MP-183A calibration, noise-diode injection is used to measure the system gain continuously. The receiver temperature is measured once per observation cycle using an internal black-body target. The noise-diode effective temperature is calibrated once every few months using an external liquid-nitrogen target, leading to an estimated accuracy of about $\sim$1 K depending on the channel [12].

D. Radiosondes

At the ARM NSA site, two daily operational radiosonde launches are performed routinely. During the three weeks of RHUBC, the operational radiosonde observations (RAOBs) were complemented by a large number of additional radiosondes that were released only during clear sky and very low water vapor content. These favorable conditions were detected continuously (24/7) using near-real-time GSR retrievals. A total of 94 radiosondes were launched, of which 38 were later judged as clear sky according to simultaneous ceilometer data. All radiosondes launched during RHUBC are RS92 manufactured by Vaisala.

Although the radiosondes offer the best available information on temperature and humidity profiles during RHUBC, it is well known that radiosonde humidity profiles may contain inaccuracies. Several studies have been performed to quantify and correct radiosonde humidity biases at low to midlatitudes [13], [17]–[19], but this is more difficult to assess in polar regions [9], [15], [16]. In fact, radiosonde measurements are inherently less accurate for dry, rather than moist, conditions, but the absolute accuracy is far more difficult to assess. For example, bias corrections based on humidity profile scaling by the IWV measured by microwave radiometers operating at K-band frequencies (20–30 GHz) [18] are not generally applicable in the Arctic due to lack of sensitivity of this conventional instrumentation [2]–[4]. On the other hand, the bias correction based on solar zenith angle [17] would be small ($\sim$2%) during the low solar illumination of polar winter. It is important to note that bias corrections are not error free; as an example, systematic errors in the bias correction described in [16] are estimated to be 2%–3%. However, the Vaisala RS92 humidity measurements have been tested with respect to a reference-quality hygrometer of known accuracy [19] and found to be the most accurate operational radiosonde tested. In the same analysis, it is shown that RS92 humidity soundings, without any correction, agree with the reference within 2% in the lower troposphere and 3% in the middle to upper troposphere. Since the uncertainty associated with bias correction may be of the

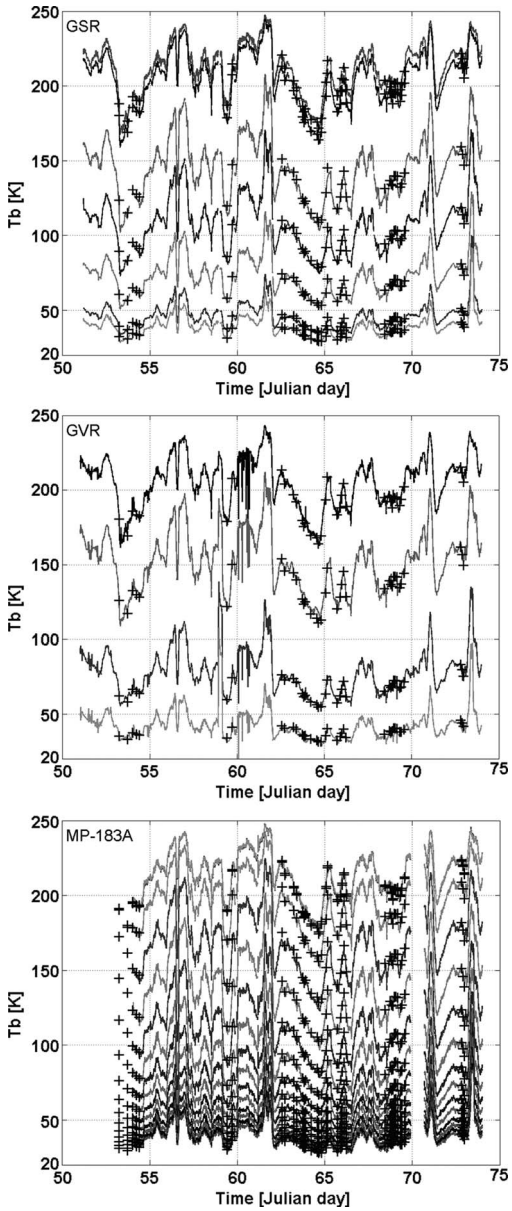

Fig. 1. Time series of Tb as observed by GSR, GVR, and MP-183A during RHUBC. Black cross indicates the simulated Tb based on clear-sky RAOB following [6]. In each panel, Tb time series distribute from top to bottom (higher to lower values) corresponding to channels from top to bottom of Table I (going from opaque to transparent).

same order as the errors expected from RS92, no bias correction was applied to the radiosoundings used in this paper.

The experiment-long time series of Tbs observed by GSR, GVR, and MP-183A 183.31-GHz channels is shown in Fig. 1, together with the associated Tb simulations computed from clear-sky RAOBs. The radiosonde profiles were quality checked, then extended up to 30 km with polar winter climatology, and finally processed using the MonoRTM v3.3 [6] to obtain Tbs.

III. Comparison of Independent Observations

As shown in Table I, the GSR, GVR, and MP-183A have very similar channels in the vicinity of the 183.31-GHz water vapor line. This fortunate situation gives us the opportunity to compare colocated independent observations and, thus, to evaluate the relative performances of the three instruments. As discussed in Section I, different design characteristics preclude direct comparison of Tb. However, these differences can be predicted indirectly in Tb space once the hardware characteristics are properly modeled. For example, the MP-183A channels are all single sideband, while both GSR and GVR have double-sideband channels. Since the 183.31-GHz absorption line is not exactly symmetrical, we expect differences on the order of few kelvins between single- and double-sideband channels. The underlying assumption is that the channels are similar enough that one can predict the Tb differences accurately from simulated data, without the need to consider spectral issues related to absorption models, radiosonde biases, etc. This approach has been frequently used for instrument intercomparison ([20] and references therein).

Therefore, for each clear-sky RAOB, the expected Tbs were calculated for the entire set of channels (7 for the GSR, 4 for the GVR, and 15 for the MP-183A), taking into account the relevant instrument characteristics (central frequency, sideband, bandwidth, spectral response function) and band averaging. To compute Tb, we used the MonoRTM v3.3 forward model [7] with the recent modifications in the air-broadened half widths of 22- and 183-GHz water vapor lines, as discussed in [6]. Note that part of these modifications were determined by comparison between simulations (using the MonoRTM v3.0) and a larger set of GVR observations at ARM NSA from January to October 2007, spanning a wider range of IWV conditions than encountered during RHUBC. Profiles of trace gases, as well as temperature, humidity, and pressure, above the uppermost radiosonde altitude were represented using climatological profiles. Moreover, humidity readings leading to unrealistic volume-mixing-ratio values above 9 km were set to climatological values. Monochromatic calculations were performed at 100-MHz intervals over the specified bandpass widths for the GVR, using the passband-filter function in [5], at 12 points per channel over the specified bandpass for MP-183A and at the estimated EMFs for the GSR. Radiances were calculated at each interval and, then, averaged before converting to Tb. A few typical examples are shown in Fig. 2, where Tb from four GVR (183.31 ± 1, 3, 7, and 14 GHz) and MP-183A (182, 180, 176, and 170 GHz) channels are plotted against Tb from the corresponding nearest GSR channels (183.31 ± 1, 3.05, 7, and 16 GHz). Comparison of both observed and simulated data sets are shown; note that, due to the different channel characteristics, neither the observed nor simulated comparisons are expected to lie on the $1:1$ line. If the instruments were all in perfect agreement, the line fitted through the measurement/measurement points would be exactly the same as the line fitted through the model/model points for each pair of channels. For most of the comparisons shown in Fig. 2, the observed Tbs lie nicely over the simulations. Conversely, there are cases in which the comparison significantly departs from model prediction, as in GVR 183.31 ± 3 GHz versus GSR 183.31 ± 3.05 GHz and GVR 183.31 ± 14 GHz versus GSR 183.31 ± 16 GHz. Similar scatter plots were produced for all the independent channel pairs with similar spectral characteristics,

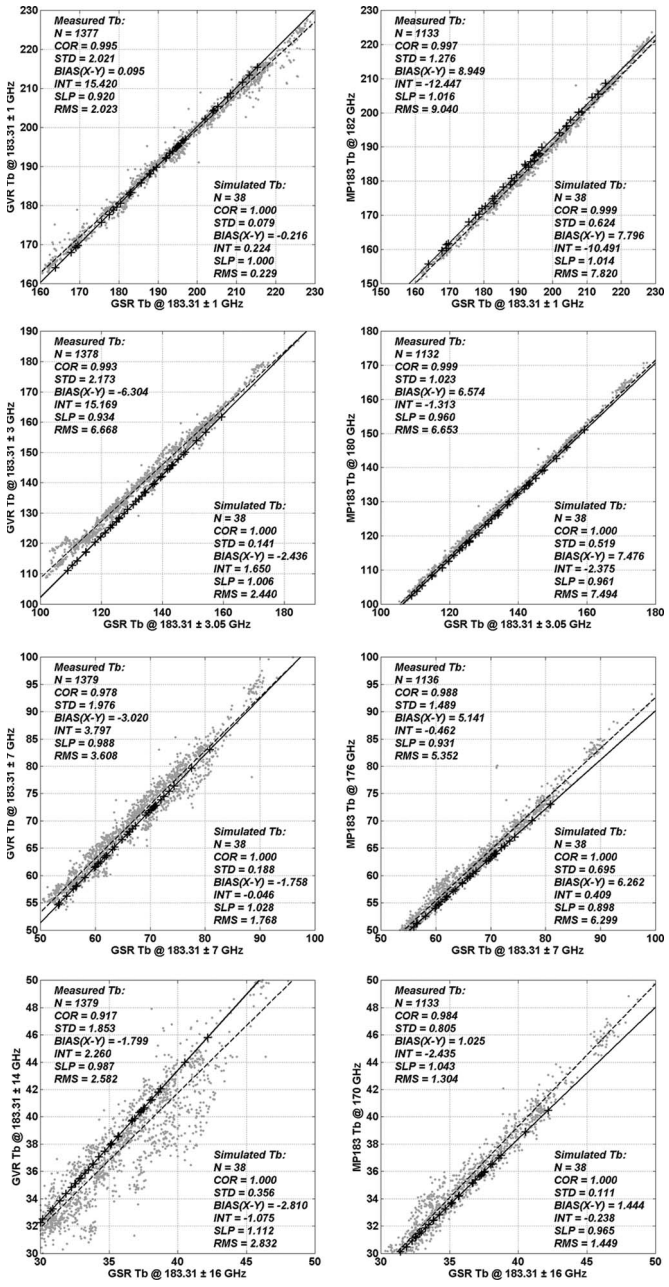

Fig. 2. Scatter plot of Tb from selected GVR and MP-183A channels versus GSR Tb at corresponding nearest channels (gray dots). Black crosses indicate the simulated Tb based on clear-sky RAOB. Lines show linear fit through (dashed) observations and (continuous) simulations. Statistics extracted from measured and simulated data sets are given in the upper left and the lower right corners, respectively. Note that Tbs are not expected to lie over the 1 : 1 diagonal, due to different channels' characteristics. Perfect agreement between the different measurements would result in the dashed line overlaying the solid line.

leading to the statistics summarized in Table II. We see that systematic differences between the channel pairs are generally explained by the different hardware specification. In fact, apart from GVR 183.31 ± 3 GHz versus GSR 183.31 ± 3.05 GHz and GVR 183.31 ± 3 GHz versus MP-183A 180 GHz pairs, the experimental bias remains within 1.5 K from the simulation predictions, consistently with an $\sim$1 K absolute accuracy for each instrument. Considering the standard deviation of the residuals in Table II, these are for each pair within the

TABLE II
STATISTICS OF CLEAR-SKY TB RESIDUALS BETWEEN INDEPENDENT CHANNEL PAIRS AS OBSERVED (BOLD, SAMPLE $>$ 1000) AND MODELED (PLAIN, SAMPLE $=$ 38) DURING RHUBC 2007

CHN PAIR (GHz)	BIAS (K)	STD (K)	RMS (K)	COR	P(1)	P(0) (K)
GVR 183±1	**0.09**	**2.02**	**2.02**	**0.99**	**0.92**	**15.42**
GSR 183±1	-0.22	0.08	0.23	1.00	1.00	0.22
MP-183A 182	**8.95**	**1.28**	**9.04**	**1.00**	**1.02**	**-12.45**
GSR 183±1	7.80	0.62	7.82	1.00	1.01	-10.49
GVR 183±3	**-6.30**	**2.17**	**6.67**	**0.99**	**0.93**	**15.17**
GSR 183±3	-2.44	0.14	2.44	1.00	1.00	1.65
MP-183A 180	**6.56**	**1.02**	**6.65**	**1.00**	**0.96**	**-1.31**
GSR 183±3	7.48	0.52	7.49	1.00	0.96	-2.37
GVR 183±7	**-3.02**	**1.98**	**3.61**	**0.98**	**0.99**	**3.80**
GSR 183±7	-1.76	0.19	1.77	1.00	1.03	-0.05
MP-183A 176	**5.14**	**1.49**	**5.35**	**0.99**	**0.93**	**-0.46**
GSR 183±7	6.26	0.69	6.30	1.00	0.90	0.41
GVR 183±14	**-1.80**	**1.85**	**2.58**	**0.92**	**0.99**	**2.26**
GSR 183±16	-2.81	0.36	2.83	1.00	1.11	-1.07
MP-183A 170	**1.02**	**0.80**	**1.30**	**0.98**	**1.04**	**-2.43**
GSR 183±16	1.44	0.11	1.45	1.00	0.96	-0.24
MP-183A 182	**8.67**	**2.47**	**9.01**	**0.99**	**1.07**	**-23.33**
GVR 183±1	8.01	0.70	8.04	1.00	1.01	-10.66
MP-183A 180	**12.91**	**2.05**	**13.0**	**0.99**	**1.02**	**-15.30**
GVR 183±3	9.91	0.64	**8** 9.93	1.00	0.95	-3.92
MP-183A 176	**7.93**	**1.86**	**8.14**	**0.98**	**0.89**	**-0.50**
GVR 183±7	8.02	0.88	8.07	1.00	0.87	0.45
MP-183A 170	**2.51**	**1.63**	**2.99**	**0.93**	**0.87**	**2.55**
GVR 183±14	4.25	0.47	4.28	1.00	0.87	0.70

expectations for a comparison of two independent variables with an accuracy of $\sim$1–2 K. Finally, Table II also reports correlation coefficients equal or greater than 0.98 for all but the pairs involving GVR 183.31 ± 14 and slopes of linear fit within 8% with respect to simulations, besides for the GVR 183.31 ± 14 GHz versus GSR 183.31 ± 16 GHz pair. From all these considerations, we can conclude that the comparative analysis of independent observations demonstrated that the majority of channels performed within the expected uncertainty. The few cases in which this is not strictly true all involve either the GVR 183.31 ± 3-GHz or the GVR 183.31 ± 14-GHz channels, suggesting a potential problem with their calibration. This will be discussed in the next section.

Considering the high sensitivity of 183-GHz channels to IWV [6] and the level of consistency between most of the channels in Table II, it follows that there should be a high level of expected accuracy for IWV estimates. For example, GSR 183 ± 7-, GVR 183 ± 7-, and MP-183A 170-GHz channels agree within 1.3 K with respect to model expectations; assuming the sensitivity of these channels to be $\sim$30 K/mm [6], this leads to IWV expected uncertainties of 0.04 mm, roughly 4% of the values of RHUBC interest (1 mm). Applying the same considerations to GSR 183 ± 3 GHz and MP-183A 180 GHz, with a sensitivity of $\sim$70 K/mm [6], the expected uncertainties are reduced to less than 2%.

IV. COMPARISON WITH SIMULATIONS

The RHUBC data set provides a unique basis for evaluating both models and measurements in the vicinity of the 183.31-GHz line. Since the spectral characteristics of the channels have been properly modeled, the observed Tbs can also be directly compared with simulated Tbs. Assuming that the observations from the three instruments are consistent (i.e., the accuracy for all channels is within specifications), this analysis should quantify the agreement between model

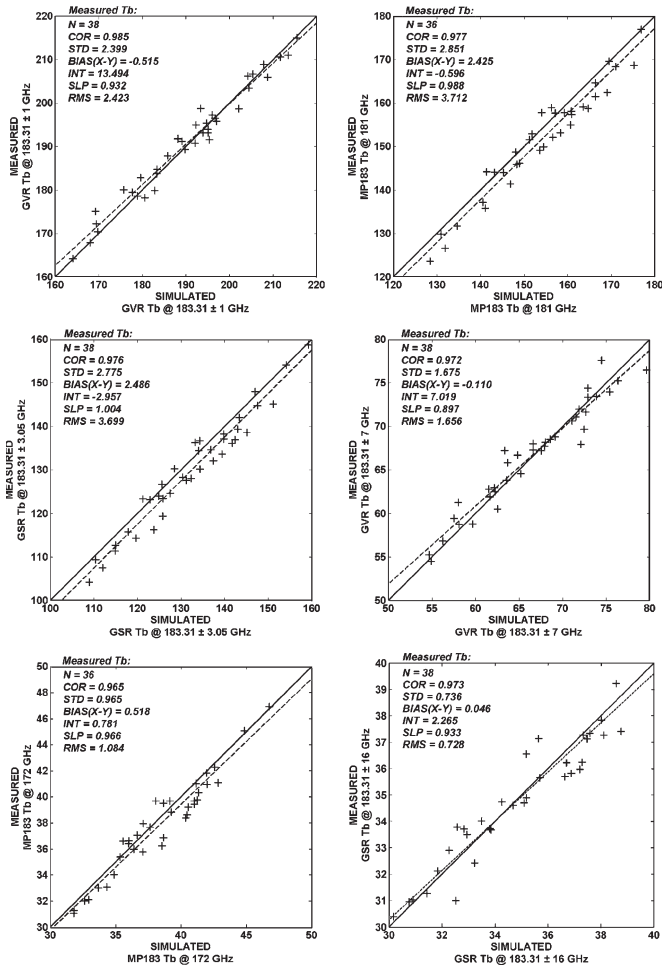

Fig. 3. Measured versus simulated Tb from selected GSR, GVR, and MP-183A channels. The black solid line represents the 1 : 1 line, while the dashed line shows the linear fit.

and observations and indicate possible frequency-dependent signatures from systematic errors in the radiosonde profiles or the model. Note that, in contrast to the results in [10], in this paper, the GVR simulations have been reprocessed, accounting for the measured filter function (as described earlier), and the GVR observations have been recalibrated in radiance and then converted to Tb to be consistent with the simulations. In order to compare equal numbers of measured and simulated points, the radiometer measurements were averaged over a time period from 5 min before to 30 min after each radiosonde launch, to account for the time taken for the radiosonde to reach its upper measurement altitude. Few examples and a summary of the statistics obtained from the set of 38 matchups of observations and clear-sky RAOB simulations are given in Fig. 3 and Tables III–V, respectively. Besides the other considerations discussed as follows, note that the slopes P(1) of the model/measurement comparison are always within 10% except for the GVR 183.31 ± 14-GHz channel. An inconsistency between this and other GVR channels was already noticed by Payne *et al.* [6], suggesting a problem either with the calibration or with the modeling of the 183.31 ± 14-GHz channel. From our results, the slopes given by similar independent channels from the other two radiometers (e.g., GSR 183.31 ± 12 and 16 GHz, MP-183A 170 and 171 GHz) are much closer to one,

TABLE III
STATISTICS OF CLEAR-SKY TB RESIDUALS (SIMULATED MINUS OBSERVED) FOR GSR DURING RHUBC 2007 (SAMPLE = 38). FROM LEFT TO RIGHT, COLUMNS SHOW THE CHANNELS (CHN), MEAN VALUE (BIAS), STANDARD DEVIATION (STD), ROOT MEAN SQUARE (RMS), CORRELATION COEFFICIENT (COR), SLOPE (P(1)), AND INTERCEPT (P(0)) OF A LINEAR FIT

CHN (GHz)	BIAS (K)	STD (K)	RMS (K)	COR	P(1)	P(0) (K)
183.31 ± 0.55	-1.81	2.74	3.25	0.98	0.98	5.06
183.31 ± 1.0	-0.78	2.72	2.79	0.98	0.99	2.72
183.31 ± 3.05	2.49	2.78	3.70	0.98	1.00	-2.96
183.31 ± 4.7	1.76	2.40	2.95	0.97	1.02	-3.35
183.31 ± 7.0	0.68	1.63	1.75	0.97	0.97	1.30
183.31 ± 12	1.22	0.93	1.53	0.97	0.94	1.29
183.31 ± 16	0.05	0.74	0.73	0.97	0.93	2.27

TABLE IV
AS IN TABLE II BUT FOR GVR (SAMPLE = 38)

CHN (GHz)	BIAS (K)	STD (K)	RMS (K)	COR	P(1)	P(0) (K)
183.31 ± 1.0	-0.51	2.40	2.42	0.98	0.93	13.49
183.31 ± 3.0	-1.76	2.81	3.29	0.98	0.89	15.96
183.31 ± 7.0	-0.11	1.67	1.66	0.97	0.90	7.02
183.31 ± 14.0	1.47	1.79	2.30	0.86	0.74	8.34

TABLE V
AS IN TABLE II BUT FOR MP-183A (SAMPLE = 38)

CHN (GHz)	BIAS (K)	STD (K)	RMS (K)	COR	P(1)	P(0) (K)
183.31	-1.91	2.61	3.21	0.98	0.95	12.73
183.00	-1.86	2.53	3.11	0.98	0.98	6.73
182.00	0.43	2.69	2.68	0.98	0.98	3.97
181.00	2.42	2.85	3.71	0.98	0.99	-0.60
180.00	1.41	2.51	2.85	0.98	0.96	6.74
179.00	0.90	2.15	2.30	0.98	1.01	-1.70
178.00	0.29	1.99	1.99	0.97	1.00	-0.61
177.00	0.40	1.70	1.73	0.97	0.99	0.02
176.00	-0.47	1.31	1.38	0.98	0.99	1.23
175.00	-0.50	1.98	2.01	0.94	1.00	0.41
174.00	-0.32	1.18	1.21	0.97	1.02	-0.83
173.00	0.36	0.95	1.00	0.98	1.03	-1.67
172.00	0.52	0.97	1.08	0.97	0.97	0.78
171.00	0.18	0.86	0.87	0.97	0.99	0.13
170.00	-0.31	0.75	0.81	0.97	1.00	0.37

thus indicating that a calibration error is likely the cause of the model/measurement differences at 183.31 ± 14 GHz. However, a residual effect related to inaccurate modeling of the passband filter cannot be excluded at this time, since the GVR filter shapes used in the calculation were derived from measurements performed on an identical, although independent, unit, as aforementioned in Section II-B.

As shown in Fig. 4, Tb residuals (simulated minus observed) for GSR, GVR, and MP-183A channels are plotted against simulated Tb. Note that each panel shows Tb from all the channels belonging to the associated instrument, without spectral distinction. In addition, Fig. 5 shows the bias and one standard (also given in Tables III–V) for each channel of the three instruments plotted against the channels' spectral displacement from the line center (183.31 GHz).

Tables III–V show residuals within 3.7-K rms for all the instruments, with small biases. The observed scatter on the model/measurement comparisons is unlikely to be dominated by radiometer noise, since the radiometer measurements are 35-min averages. It is more likely that most of the scatter is due to sonde-to-sonde variability in the radiosonde humidity-measurement error and/or the fact that the radiosonde is not

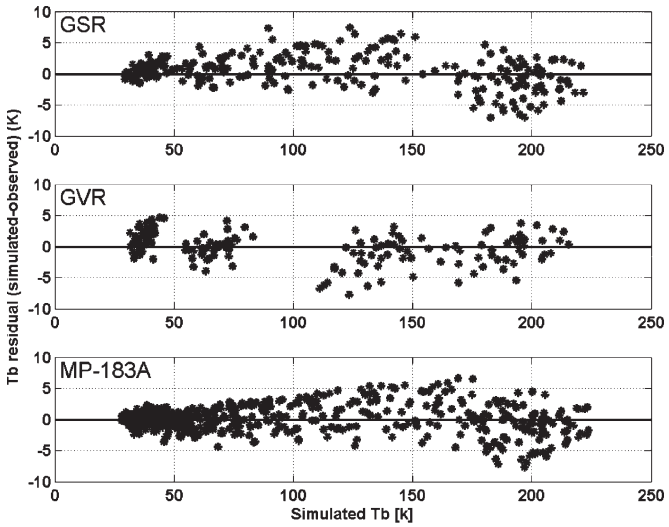

Fig. 4. Tb residuals (simulated minus observed) for GSR, MP-183A, and GVR versus Tb simulated from clear-sky RAOB for all channels.

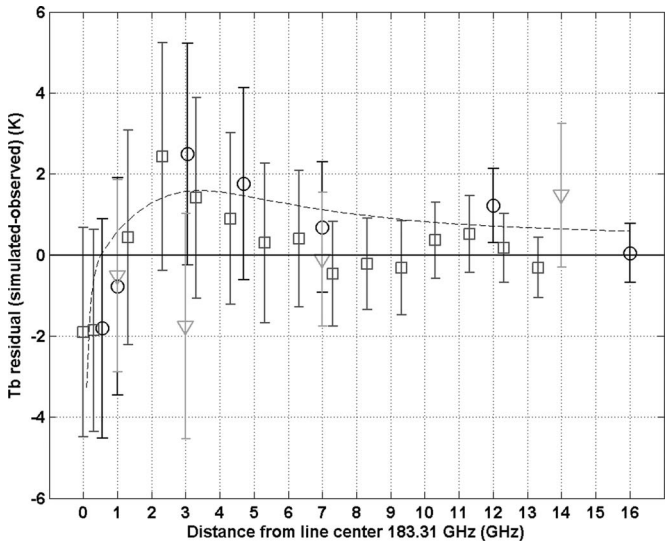

Fig. 5. Tb residuals (simulated minus observed) for (circles) GSR, (triangles) GVR, and (squares) MP-183A versus channels' spectral displacement from line center (183.31 GHz). Markers show the mean residual while error bars indicate ± 1 standard (computed over the set of 38 clear-sky RAOBs). The dashed line indicates calculated Tb differences associated with realistic sensor humidity uncertainty affecting the sounding in an opposite way at lower and upper levels (5% drier above and wetter below a reference level fixed arbitrarily to 3 km).

sampling exactly the same atmosphere as is being viewed by the radiometer. (Previous studies—for example, [6], [18]—have used the approach of scaling the IWV of radiosonde profiles to reduce such scatter as well as in addressing biases.) However, certain systematic features are observed in the comparison, which appear similar for the GSR and MP-183A but somewhat different for the GVR. Of course, part of the residuals is related to uncertainty in the instrumental characteristic specifications and their nonperfect modeling. However, we estimate that the bandpass modeling errors are well within the instrument noise level. In addition, it seems unlikely that calibration or hardware uncertainties cause similar features in independent instruments. Fig. 5 shows that the three instruments agree with MonoRTM within 1.5 K for the most transparent channels (i.e., displacement larger than 5 GHz). For the most opaque channels, roughly within 1 GHz from the line center (i.e., GSR chn#1, MP-183A chn#14–15), GSR and MP-183A residuals show a consistent -2-K bias, which could be explained considering radiosonde errors in sensing moisture in the upper atmosphere [8], [9]. In fact, in very dry conditions, these channels are sensitive to upper troposphere–lower stratosphere humidity [2], [8], [9], which is not always accurately represented by radiosonde sensors or climatological profiles. Note that the GVR does not have channels this close to the line center and, therefore, has no comparable points in Fig. 5.

For channels with intermediate opacity, for example, from 2 to about 8 GHz from the line center, residuals for GSR and MP-183A again agree well within each other and seem to show similar variations with frequency. The GVR 183.31 ± 7-GHz channel appears to agree with the other two instruments in this respect, but the GVR 183.31 ± 3-GHz channel is clearly anomalous. Radio-frequency interference (RFI) from a nearby naval base was observed during the experiment. Of all instruments and channels, the GVR ± 3-GHz channel was found to be the most sensitive to RFI. Although RFI mitigation processing is applied to GVR data operationally, we suspect that the anomalous result from this channel is related to problems with the filtering of the data. Note that channels ~ 3 GHz apart from the line center are the least sensitive of all to the recent modifications in the air-broadened half widths of the 183-GHz water vapor line [6]. Analysis of GVR channels under moister conditions, where the channels become opaque and therefore insensitive to any model input other than local temperature, point to substantial instrument calibration offsets in some of the GVR channels. For the low IWV conditions during RHUBC, it is difficult to assess instrument offsets independently of systematic errors in radiosonde humidity.

Fig. 5 shows a common spectral variation in the GSR and MP-183A residuals. The shape and magnitude of the residuals cannot be accounted for by spectroscopic parameters in the model (linewidth, line strength, or water-vapor continuum). Forward-model calculations show that if the line strength is changed by 5% and the width by about 3%, then the spectral feature of residuals could be removed. However, it is believed that the line strength is known to the 1% accuracy ([7] and references therewith), and thus, a 5% change is not likely. Due to the dry conditions, an error in the self-broadened water-vapor continuum would have negligible effect on the residuals. An error in the foreign-broadened water-vapor continuum would result in a spectral signature that would increase with distance from the line center, while Fig. 5 shows a decrease in the residuals with distance from the line center. Therefore, the water-vapor continuum uncertainty alone could not explain the observed spectral signature. It may be possible that spectral shifts in instrument channels may explain this spectral residual, but it is unlikely that both the MP-183 (single sideband) and GSR (double sideband) would show the same spectral residual. Therefore, we believe that the most likely source of model-related uncertainty is the radiosonde humidity profiles used as input. In particular, the shape of the residuals, changing sign with distance from line center, would suggest a radiosonde error of opposite sign in the lower and upper atmospheres. In qualitative support of this speculation, Fig. 5 also shows

the calculated Tb differences associated with realistic sensor humidity uncertainty affecting the sounding in an opposite sense at lower and upper levels. This residual was obtained by computing Tb with a reference sounding and then subtracting the Tb computed using the same sounding modified to be 5% drier above and 5% wetter below the 3-km altitude. Note that we have arbitrarily chosen values that best fit the error bars, which resulted in slightly lower IWV.

This height dependence of the radiosonde bias is a hypothesis supported by the smaller likelihood of other sources that could cause the observed spectral dependence of the residuals (i.e., the line strength and spectral shift of the radiometers). This hypothesis seems consistent with the findings in [14], [16], and [19]. In fact, Newsom *et al.* [14] have shown comparison of RS92 with Raman lidar observations at a midlatitude continental location (ARM Southern Great Plains site, Lamont, OK, U.S.) which seems to agree with our hypothesis, although with smaller magnitude. Miloshevich *et al.* [19], comparing RS92 with reference-quality hygrometer, report up to 2% wet bias in the lower troposphere during dry conditions and 0%–4% dry bias in the medium to upper troposphere. Finally, in a polar environment (Antarctica), Rowe *et al.* [16] compared RS90 soundings with ground-based interferometric infrared observation and found consistently dry bias in a range of pressures from 650 to 200 mb ($\sim$3–10 km). While extensive studies have been performed to determine radiosonde biases, from the tropics [13], [17]–[19] to the poles [15], [16], radiosonde height-dependent uncertainties are as yet not well quantified, particularly at polar regions during extremely dry conditions [9]. Although it is beyond the scope of this paper, it would be interesting to apply the empirical correction in [19] (obtained from RS92 launched at midlatitude) to the set of Arctic radiosondes used in this paper. Since this correction tends to decrease radiosonde humidity in the lower troposphere (in dry conditions) and increase humidity in the upper troposphere, we expect it to mitigate the residual spectral behavior in Fig. 5.

V. Conclusion

Three millimeter-wave radiometers (GSR, GVR, and MP-183A), with channels around the 183.31-GHz water vapor line, were operated during the RHUBC experiment. During RHUBC, the air temperature (at 2 m) ranged from -38 °C to -19 °C and IWV content from 0.9 to 3.6 mm. Therefore, RHUBC provided the opportunity to compare colocated independent observations during extremely dry and cold conditions, evaluating the relative performances of the three instruments and comparing with forward-model simulations. Simulations have been computed from Vaisala RS92 RAOBs during clear sky (as detected by a colocated ceilometer) using version 3.3 of the MonoRTM code (which includes recent linewidth modifications [6]).

In general, the instrument cross-validation performed for sets of channel pairs, taking into account the different spectral characteristics, showed agreement within the total expected uncertainty. The consistency between instruments allows the determination of the IWV to within around 2% for these dry conditions. However, spectral features were found by investigating Tb residuals (simulated minus observed), indicating some degree of inconsistency between the instruments and the forward model. The most likely cause of forward-model error is systematic errors in the radiosonde humidity profiles used as input and could be further investigated using hyperspectral infrared observations from colocated ground-based interferometer [13], [16] or lidar [14].

Acknowledgment

The data used in this paper were collected as part of the ARM Program sponsored by the U.S. DOE, Office of Science, Office of Biological and Environmental Research, Climate and Environmental Sciences Division.

References

[1] T. P. Ackerman and G. M. Stokes, "The Atmospheric Radiation Measurement program," *Phys. Today*, vol. 56, no. 1, pp. 38–44, Jan. 2003.

[2] D. Cimini, E. R. Westwater, A. J. Gasiewski, M. Klein, V. Ye Leuski, and J. C. Liljegren, "Ground-based millimeter- and submillimeter-wave observations of low vapor and liquid water contents," *IEEE Trans. Geosci. Remote Sens.*, vol. 45, no. 7, pp. 2169–2180, Jul. 2007.

[3] M. P. Cadeddu, J. C. Liljegren, and A. L. Pazmany, "Measurements and retrievals from a new 183-GHz water-vapor radiometer in the Arctic," *IEEE Trans. Geosci. Remote Sens.*, vol. 45, no. 7, pp. 2217–2223, Jul. 2007.

[4] D. Cimini, E. R. Westwater, A. J. Gasiewski, M. Klein, V. Y. Leuski, and S. G. Dowlatshahi, "The ground-based scanning radiometer: A powerful tool for study of the arctic atmosphere," *IEEE Trans. Geosci. Remote Sens.*, vol. 45, no. 9, pp. 2759–2777, Sep. 2007.

[5] A. L. Pazmany, "A compact 183-GHz radiometer for water vapor and liquid sensing," *IEEE Trans. Geosci. Remote Sens.*, vol. 45, no. 7, pp. 2202–2207, Jul. 2007.

[6] V. H. Payne, J. S. Delamere, K. E. Cady-Pereira, R. R. Gamache, J.-L. Moncet, E. J. Mlawer, and S. A. Clough, "Air-broadened half-widths of the 22 GHz and 183 GHz water vapor lines," *IEEE Trans. Geosci. Remote Sens.*, vol. 46, no. 11, pp. 3601–3617, Nov. 2008.

[7] S. A. Clough, M. W. Shephard, E. J. Mlawer, J. S. Delamere, M. J. Iacono, K. Cady-Pereira, S. Boukabara, and P. D. Brown, "Atmospheric radiative transfer modeling: A summary of the AER codes," *J. Quant. Spectrosc. Radiat. Transf.*, vol. 91, no. 2, pp. 233–244, Mar. 2005.

[8] P. E. Racette, E. J. Kim, J. R. Wang, E. R. Westwater, M. Klein, V. Leuski, Y. Han, A. J. Gasiewski, D. Cimini, D. C. Jones, W. Manning, and P. Kiedron, "Measuring low amounts of precipitable water vapor using millimeterwave radiometry," *J. Atmos. Ocean. Technol.*, vol. 22, no. 4, pp. 317–337, Apr. 2005.

[9] V. Mattioli, E. R. Westwater, D. Cimini, A. J. Gasiewski, M. Klein, and V. Y. Leuski, "Microwave and millimeter-wave radiometric and radiosonde observations in an arctic environment," *J. Atmos. Ocean. Technol.*, vol. 25, no. 10, pp. 1768–1777, Oct. 2008.

[10] D. Cimini, F. Nasir, E. R. Westwater, V. H. Payne, D. D. Turner, E. J. Mlawer, and M. L. Exner, "Comparison of ground-based millimeter-wave observations in the Arctic winter," in *Proc. Microrad*, Firenze, Italy, Mar. 11–14, 2008, pp. 1–4.

[11] D. Cimini, E. R. Westwater, A. J. Gasiewski, M. Klein, and V. Leuski, "Temperature and humidity profiling in the Arctic using millimeter-wave radiometry," in *Proc. Microrad*, Firenze, Italy, Mar. 11–14, 2008, pp. 1–4.

[12] M. Exner, private communication.

[13] E. R. Westwater, B. B. Stankov, D. Cimini, Y. Han, J. A. Shaw, B. M. Lesht, and C. N. Long, "Radiosonde humidity soundings and microwave radiometers during Nauru99," *J. Atmos. Ocean. Technol.*, vol. 20, no. 7, pp. 953–971, Jul. 2003.

[14] R. Newsom, D. D. Turner, B. Mielke, M. Clayton, and R. Ferrare, "The use of simultaneous analog and photon counting detection for Raman lidar," *Appl. Opt*. (in press).

[15] V. Mattioli, E. R. Westwater, D. Cimini, J. S. Liljegren, B. M. Lesht, S. I. Gutman, and F. J. Schmidlin, "Analysis of radiosonde and ground-based remotely sensed PWV data from the 2004 north slope of Alaska arctic winter radiometric experiment," *J. Atmos. Ocean. Technol.*, vol. 24, no. 3, pp. 415–431, Mar. 2007.

[16] P. M. Rowe, L. M. Miloshevich, D. D. Turner, and V. P. Walden, "Dry bias in Vaisala RS90 radiosonde humidity profiles over Antarctica," *J. Atmos. Ocean. Technol.*, vol. 25, no. 9, pp. 1529–1541, Sep. 2008.
[17] K. Cady-Pereira, M. W. Shephard, D. D. Turner, E. J. Mlawer, S. A. Clough, and T. J. Wagner, "Improved daytime column-integrated precipitable water vapor from Vaisala radiosonde humidity sensors," *J. Atmos. Ocean. Technol.*, vol. 25, no. 6, pp. 873–883, Jun. 2008.
[18] D. D. Turner, B. M. Lesht, S. A. Clough, J. C. Liljegren, H. E. Revercomb, and D. C. Tobin, "Dry bias and variability in Vaisala radiosondes: The ARM experience," *J. Atmos. Ocean. Technol.*, vol. 20, no. 1, pp. 117–132, Jan. 2003.
[19] L. M. Miloshevich, H. Vömel, D. N. Whiteman, B. M. Lesht, F. J. Schmidlin, and F. Russo, "Absolute accuracy of water vapor measurements from six operational radiosonde types launched during AWEX-G, and implications for AIRS validation," *J. Geophys. Res.*, vol. 11, p. D09 S10, Apr. 2006. DOI:10.1029/2005JD006083.
[20] D. Cimini, E. R. Westwater, Y. Han, and S. J. Keihm, "Accuracy of ground-based microwave radiometer and balloon-borne measurements during WVIOP2000 field experiment," *IEEE Trans. Geosci. Remote Sens.*, vol. 41, no. 11, pp. 2605–2615, Nov. 2003.

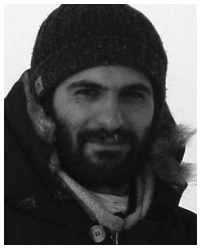

Domenico Cimini received the Laurea (*cum laude*) and Ph.D. degrees in physics from the University of L'Aquila, L'Aquila, Italy, in 1998 and 2002, respectively.

From 2002 to 2004, he was with the Center of Excellence for Remote Sensing and Modeling of Severe Weather (CETEMPS), University of L'Aquila. From 2004 to 2005, he was a Visiting Fellow in the Cooperative Institute for Research in Environmental Sciences, University of Colorado at Boulder (CU), Boulder. From 2005 to 2006, he was with the Institute of Methodologies for the Environmental Analysis, Italian National Research Council, where he worked on ground- and satellite-based observations of cloud properties. Since 2006, he has been with the Center for Environmental Technology, Department of Electrical and Computer Engineering, CU, where since 2007, he has been an Adjunct Professor. He is currently a Researcher with CETEMPS, where he is working on ground- and satellite-based passive microwave and infrared radiometry.

Dr. Cimini was recipient of the *Fondazione Ugo Bordoni Award* 2008 in memory of Prof. Giovanni D'Auria.

Francesco Nasir was born in Watford, U.K., in 1980. He received the B.Sc. degree in physics from the University of Cagliari, Cagliari, Italy, in 2005, the Master degree from the University of Reading, Reading, U.K., and the M.S. degree with a dissertation on ground-based passive remote sensing from the University of L'Aquila, L'Aquila, Italy.

He is currently with the Astronomic Observatory of Cagliari, Cagliari, where he has been working on ground-based passive microwave radiometry for characterizing the atmosphere where the Sardinian Radio Telescope is being built.

Ed R. Westwater (SM'91–F'01) received the B.A. degree in physics and mathematics from the Western State College of Colorado, Gunnison, in 1959 and the M.S. and Ph.D. degrees in physics from the University of Colorado at Boulder (CU), Boulder, in 1962 and 1970, respectively.

From 1960 to 1995, he was with the U.S. Department of Commerce. He is currently a Research Professor with the National Oceanic Atmospheric Administration–CU Center for Environmental Technology (CET) and the Cooperative Institute for Research in Environmental Science (CIRES) and with the Department of Electrical and Computer Engineering (ECE), CU, where since 1995, he has been with CIRES and, since 2006, with CET/ECE. His research has been concerned with microwave absorption in the atmosphere, remote sensing of the atmosphere and ocean surface, microwave and infrared radiative transfer, ground- and satellite-based remote sensing by passive radiometry, and the application of mathematical inversion techniques to problems in remote sensing. He has authored or coauthored more than 290 publications.

Dr. Westwater is a member of the American Meteorological Society, American Geophysical Union, and Mathematical Association of America. He was the Chairman and Organizer of the 1992 International Specialists Meeting on Microwave Radiometry and Remote Sensing Applications (MicroRad'1992) and was a Coorganizer of the MicroRad'2001. He is the past Chairman of the International Union of Radio Science Commission F from 2000 to 2002. He served as Associate Editor of *Radio Science* from 1999 to 2002. He is currently an Associate Editor of the IEEE TRANSACTIONS ON GEOSCIENCE AND REMOTE SENSING (TGARS) and served as a Guest Editor of the TGARS Special Issue devoted to MicroRad'2004 and to MicroRad'2006. He presented the American Meteorological Society's Remote Sensing Lecture in 1997 (elected December 3, 2000). He was the recipient of the 2003 Distinguished Achievement Award from the IEEE Geoscience and Remote Sensing Society. He was the recipient of the 15th V. Vaisala Award from the World Meteorological Society in 2001.

Vivienne H. Payne received the M.Phys. degree in physics from the University of Edinburgh, Edinburgh, U.K., in 2001 and the D.Phil. degree in atmospheric physics from the University of Oxford, Oxford, U.K., in 2005, where she worked on retrievals of water vapor, methane, and their minor isotopologues from an infrared limb sounder flying on the Envisat satellite.

She was with the University of Colorado at Boulder, Boulder, where she worked on the interpretation of her limb retrievals of water-vapor isotopes. Since January 2006, she has been with the Radiation and Climate Group of the Atmospheric and Environmental Research, Inc., Lexington, MA. Her principal areas of interest are in atmospheric radiative-transfer modeling, molecular spectroscopy (in the context of atmospheric remote sensing), and retrievals in the infrared and microwave regions.

David D. Turner received the B.A. and M.S. degrees in mathematics from Eastern Washington University, Cheney, in 1992 and 1994, respectively, and the Ph.D. degree in atmospheric science from the University of Wisconsin-Madison, Madison, in 2003.

He is currently a Researcher with the Space Science and Engineering Center, University of Wisconsin-Madison. He is actively involved in the U.S. Department of Energy Atmospheric Radiation Measurement (ARM) Program, where he is currently the Chair of the ARM Radiative Processes working group and is a Member of the ARM Science Team Executive Committee. His current research interests include infrared and microwave remote sensing, long-wave radiative transfer in clear and cloudy atmospheres, and retrieving water vapor, cloud, and aerosol properties from active and passive remote sensors.

Eli J. Mlawer received the B.A. degree in mathematics and astronomy from Williams College, Williamstown, MA, in 1982, the B.A. and M.A. degrees in physics from Cambridge University, Cambridge, U.K., in 1984 and 1990, respectively, and the Ph.D. degree in physics from Brandeis University, Waltham, MA in 1994.

Since then, he has been with Atmospheric and Environmental Research, Inc., Lexington, MA, where he is the Manager of the Radiation and Climate Group and has primary responsibility for the design, implementation, and validation of RRTM, a radiative transfer model for climate applications used by many climate and weather prediction models. He is a participant in the research being conducted with a number of climate models utilizing RRTM and continues to actively partake in the Intercomparison of Radiation Codes in Climate Models effort. As part of his involvement in the U.S. Department of Energy Atmospheric Radiation Measurement (ARM) Program, he is the Focus Group Leader of the Broadband Heating Rate Profile project, an effort to compute fluxes and heating rates in clear and cloudy conditions at the ARM sites and to perform a closure analysis on these calculations using surface and satellite radiation measurements. He is the Coprincipal Investigator of the Radiative Heating in Underexplored Bands Campaign (RHUBC), ARM field experiments directed at increasing our understanding of radiative processes in spectral regions of importance to climate that are typically opaque when viewed from the ground due to water-vapor absorption. The first RHUBC took place in northern Alaska in early 2007, and a second more intensive follow-up experiment is planned for Chile in 2009. He is the Developer of the MT_CKD water-vapor continuum model, a key component in the majority of existing atmospheric radiative-transfer models. His research interests include atmospheric radiative transfer, climate study, and the characterization of molecular collisional broadening.

Michael L. Exner received the B.A. degree from the University of Colorado at Boulder, Boulder, CO.

He was the Project Engineer for the development of the MP-183A. He is currently the Vice President of Engineering with the Radiometrics Corporation, Boulder. He has over 35 years of entrepreneurial experience developing new companies and products for telecommunications and remote sensing.

Maria P. Cadeddu received the Laurea degree in physics from the University of Cagliari, Cagliari, Italy, in 1994 and the Ph.D. degree in physics from Heriot-Watt University, Edinburgh, U.K., in 2002.

Since 2005, she has been the Instrument Mentor for the U.S. Department of Energy Atmospheric Radiation Measurement Program Climate Research Facility microwave instrumentation. She is currently with the Argonne National Laboratory, Argonne, IL. Her research interests include microwave instrumentation and application of remote sensing to atmospheric research.

Dr. Cadeddu is a member of the American Geophysical Union.